JACS
JOURNAL OF THE AMERICAN CHEMICAL SOCIETY
Article
pubs.acs.org/JACS

A Ratiometric Two-Photon Fluorescent Probe Reveals Reduction in Mitochondrial H_2S Production in Parkinson's Disease Gene Knockout Astrocytes

Sung Keun Bae,[†,∥] Cheol Ho Heo,[†,∥] Dong Joo Choi,[‡,∥] Debabrata Sen,[†] Eun-Hye Joe,*[,‡] Bong Rae Cho,*[,§] and Hwan Myung Kim*[,†]

[†]Division of Energy Systems Research, Ajou University, Suwon 443-749, Korea
[‡]Department of Pharmacology/Neuroscience Graduate Program, Ajou University School of Medicine, Suwon 443-721, Korea
[§]Department of Chemistry, Korea University, Seoul 136-701, Korea

Supporting Information

ABSTRACT: Hydrogen sulfide (H_2S) is a multifunctional signaling molecule that exerts neuroprotective effects in oxidative stress. In this article, we report a mitochondria-localized two-photon probe, SHS-M2, that can be excited by 750 nm femtosecond pulses and employed for ratiometric detection of H_2S in live astrocytes and living brain slices using two-photon microscopy (TPM). SHS-M2 shows bright two-photon-excited fluorescence and a marked change in emission color from blue to yellow in response to H_2S, low cytotoxicity, easy loading, and minimum interference from other biologically relevant species including reactive sulfur, oxygen, and nitrogen species, thereby allowing quantitative analysis of H_2S levels. Molecular TPM imaging with SHS-M2 in astrocytes revealed that there is a correlation between the ratiometric analysis and expression levels of cystathionine β-synthase (CBS), the major enzyme that catalyzes H_2S production. In studies involving DJ-1, a Parkinson's disease (PD) gene, attenuated H_2S production in comparison with wild-type controls was observed in DJ-1-knockout astrocytes and brain slices, where CBS expression was decreased. These findings demonstrate that reduced H_2S levels in astrocytes may contribute to the development of PD and that SHS-M2 may be useful as a marker to detect a risk of neurodegenerative diseases, including PD.

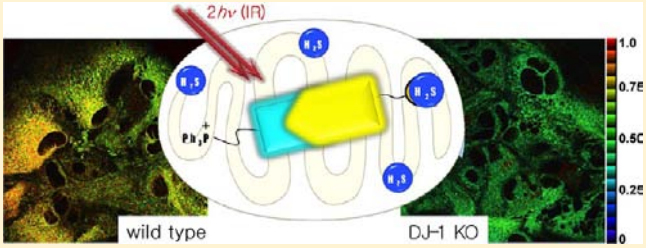

INTRODUCTION

Hydrogen sulfide (H_2S) is an endogenous signaling molecule produced by enzymes such as cystathionine β-synthase (CBS), cystathionine γ-lyase, and 3-mercaptopyruvate sulfurtransferase.[1] H_2S has diverse functions in several pathophysiological processes such as neurotransmission, modulation of redox status, neuroprotection from oxidative stress, and anti-inflammation.[2−4] Mitochondrial H_2S has been shown to exert protective effects in oxidative stress leading to dysfunction and cell death.[5−7] In the brain, there is a relatively high concentration of H_2S, and CBS, which is mainly expressed in astrocytes, has been identified as the major H_2S-producing enzyme.[8−11] Defects in H_2S production in the brain could be related to neurodegenerative diseases. Moreover, H_2S treatment protects neurons in Parkinson's disease (PD) animal models.[10,12]

In order to understand the biological and pathological roles of H_2S, monitoring of mitochondrial H_2S in live cells and tissues in normal and abnormal systems is crucial. To detect H_2S in cells, a number of fluorescent probes derived from azide,[13] an azamacrocyclic copper(II) ion complex,[14] and H_2S-specific Michael acceptors[15] have been reported. However, most of them have limitations imposed by fluorescence turn-on responses at a single detection window and/or the short excitation wavelengths required by most conventional probes. The turn-on response can vary depending on the experimental conditions, such as incident laser power and/or probe distribution, making a quantitative measurement of H_2S impossible. More recently, a mitochondrial-targeted ratiometric fluorescent probe for H_2S was also reported.[16] However, the short excitation wavelength limits its application in live-tissue imaging because of the shallow penetration depth.

An attractive approach for the detection of H_2S in live cells and tissues is ratiometric imaging with two-photon microscopy (TPM). TPM, which employs two near-IR photons as the excitation source, offers a number of advantages, including greater penetration depth (>500 μm), localization of the excitation, and longer observation times.[17−19] Therefore, there is a strong need to develop a ratiometric two-photon (TP) probe for mitochondrial H_2S.

In this work, we developed two ratiometric TP probes for mitochondrial H_2S, SHS-M1 and SHS-M2 (Scheme 1), derived from 6-(benzo[*d*]thiazol-2′-yl)-2-(methylamino)naphthalene as the fluorophore, 4-azidobenzyl carbamate as the H_2S response site,[13a] and triphenylphosphonium salt as the mitochondrial

Received: April 29, 2013
Published: June 7, 2013

   dx.doi.org/10.1021/ja404004v | *J. Am. Chem. Soc.* 2013, 135, 9915−9923

Scheme 1. Structures of SHS-M1, SHS-M2, 1, and 2

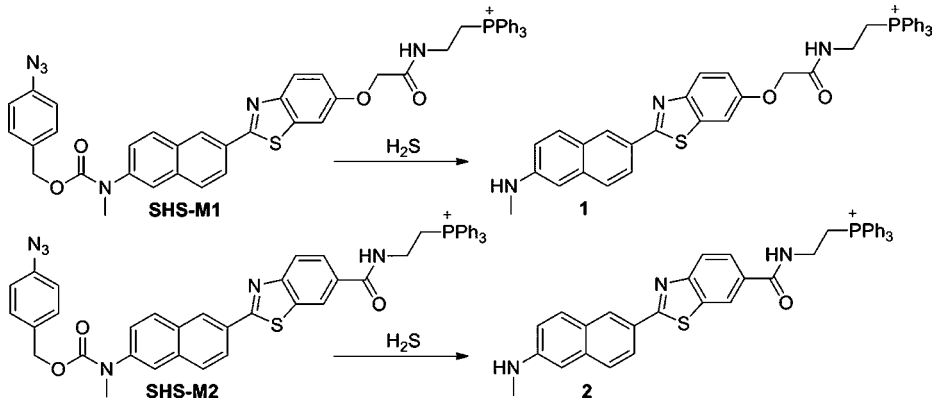

targeting moiety.[20] We anticipated that the thiolate-triggered reaction with the azide group would cleave the carbamate linkage and liberate the amino group (to give **1** and **2**, respectively), thereby shifting the emission maximum and increasing the TP cross section.[21]

RESULTS AND DISCUSSION

Spectroscopic Properties of SHS-M1 and SHS-M2. The preparation of SHS-M1 and SHS-M2 is described in the Supporting Information (SI). The solubilities of SHS-M1 and SHS-M2 in HEPES buffer (30 mM HEPES, 100 mM KCl, pH 7.4) were 3−5 μM, which was sufficient to stain the cells (Figure S1 in the SI). Under these conditions, SHS-M1 and **1** exhibited one-photon absorption maxima (λ_{abs}) at 340 nm (ε = 1.90 × 10^4 M^{-1} cm^{-1}) and 365 nm (ε = 1.80 × 10^4 M^{-1} cm^{-1}), with emission maxima (λ_{fl}) at 420 nm [fluorescence quantum yield (Φ) = 0.23] and 500 nm (Φ = 0.50), respectively (Table 1). The λ_{abs} values for SHS-M1 and SHS-M2 were nearly the same, while that of **2** was red-shifted from that of **1** by 18 nm (Figure 1 and Table 1), presumably because of the stronger electron-withdrawing group. The larger Stokes shifts observed for SHS-M2 and **2** relative to SHS-M1 and **1** can also be attributed to the greater stabilization of the charge-transfer excited state in the former two compounds, which contain a stronger electron-withdrawing group. Consistently, the emission spectra of **1** and **2** showed larger red shifts with increasing solvent polarity than the emission spectra of SHS-M1 and SHS-M2 ($\Delta\lambda_{fl}$ = 56−72 vs 16−45 nm, respectively; Figure S2 and Table S1 in the SI). Furthermore, the two-photon-excited fluorescence (TPEF) spectra of **1** and **2** measured in HeLa cells were similar to those measured in EtOH (Figure S2b,d), indicating that EtOH can adequately represent the polarity of the cellular environment.

Table 1. Photophysical Data for SHS-M1, SHS-M2, 1, and 2

compound[a]	λ_{abs} ($10^{-4}\varepsilon$)[b]	λ_{fl}[c]	Φ[d]	$\lambda^{(2)}_{max}$[e]	$\Phi\delta_{max}$[f]
SHS-M1	340 (1.9)	420	0.23 (0.41)	750	14 (32)
1	365 (1.8)	500	0.50 (1.00)	750	63 (76)
SHS-M2	343 (1.4)	464	0.24 (1.00)	740	17 (60)
2	383 (1.5)	545	0.12 (1.00)	750	55 (177)

[a]Measurements were performed in HEPES buffer (30 mM HEPES, 100 mM KCl, pH 7.4), unless otherwise noted. [b]λ_{max} of the one-photon absorption spectra in nm. The numbers in parentheses are molar extinction coefficients in M^{-1} cm^{-1} multiplied by 10^{-4}. [c]λ_{max} of the one-photon emission spectra in nm. [d]Fluorescence quantum yields, ±15%. The numbers in parentheses were measured in EtOH. [e]λ_{max} of the two-photon excitation spectra in nm. [f]Peak two-photon action cross sections in GM (1 GM = 10^{-50} cm^4 s $photon^{-1}$), ±15%. The numbers in parentheses were measured in EtOH.

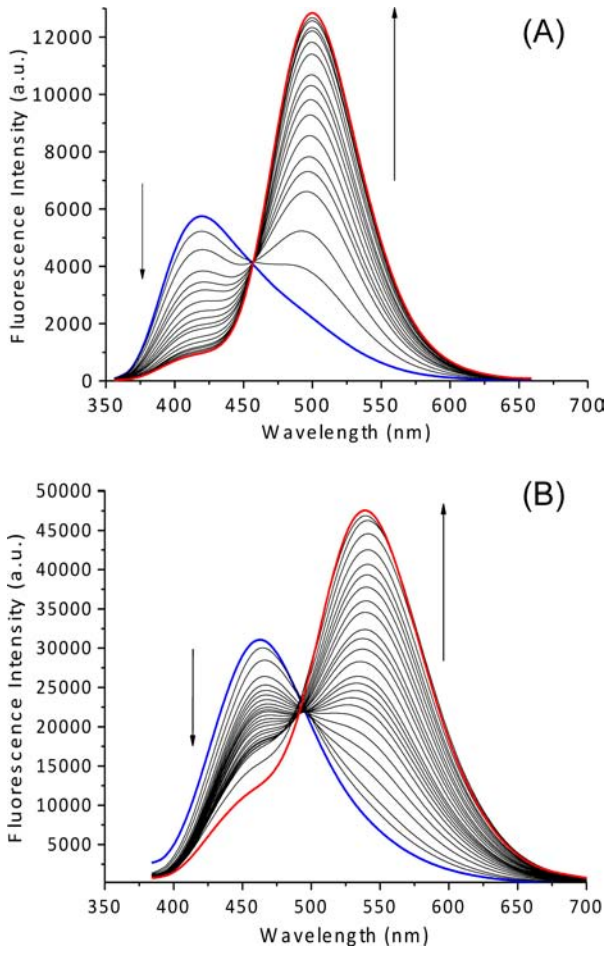

Figure 1. Fluorescence response with time for the reactions of 1 μM (A) SHS-M1 and (B) SHS-M2 with 100 μM Na_2S in HEPES buffer (30 mM HEPES, 100 mM KCl, pH 7.4). Spectra were acquired 0 to 60 min after addition of Na_2S. λ_{ex} = 340 nm (A) and 373 nm (B).

The reaction between SHS-M1 or SHS-M2 and Na_2S (a commonly employed H_2S donor)[14,15,22] produced **1** or **2**, respectively, as the only major product, as monitored by fluorescence emission (Figure 1) and LC−MS analysis (Figure S3 in the SI). In a 1 μM solution of SHS-M1 treated with 100

dx.doi.org/10.1021/ja404004v | J. Am. Chem. Soc. 2013, 135, 9915−9923

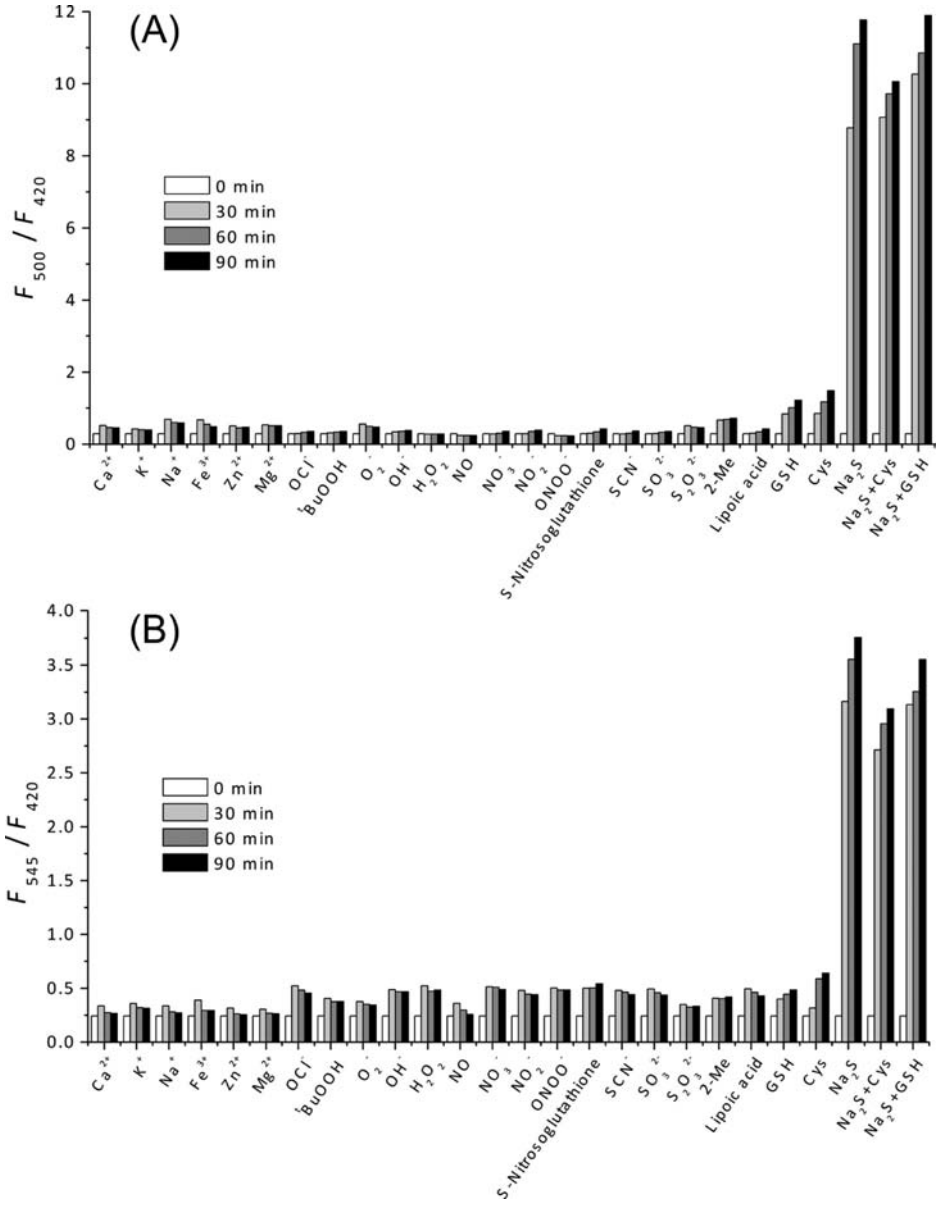

Figure 2. Fluorescence responses of 1 μM (A) SHS-M1 and (B) SHS-M2 toward 100 μM Na_2S and other reactive sulfur, nitrogen, and oxygen species as well as amino acids and metal ions. Bars represent ratios of the emission intensities at λ_{fl} at 0, 30, 60, and 90 min after addition of RSS, RNS, ROS, amino acids, or metal ions. Data were acquired in HEPES buffer (pH 7.4). λ_{ex} = 340 nm (A) and 373 nm (B).

μM Na_2S in HEPES buffer, the emission intensity increased gradually at 500 nm with a concomitant decrease at 420 nm (Figure 1a). Similar results were observed for SHS-M2, except that both λ_{fl} were significantly red-shifted (Figure 1b). These processes followed pseudo-first-order kinetics with k_{obs} = 1.4 × 10^{-3} and 9.1 × 10^{-4} s^{-1} for SHS-M1 and SHS-M2, respectively (Figure S4 in the SI). Moreover, the plots of k_{obs} versus [Na_2S] were straight lines passing through the origin (Figure S4), indicating that the reactions are overall second order with k_2 = 5.8 and 7.0 M^{-1} s^{-1} for SHS-M1 and SHS-M2, respectively. These results can be attributed to rate-limiting attack of the thiolate ion at the azide group followed by cleavage of the carbamate moiety to afford **1** or **2**, as reported.[21] Furthermore, the in vitro detection limits of H_2S with SHS-M1 and SHS-M2 were 0.2 and 0.4 μM, respectively (Figure S5 in the SI).

SHS-M1 and SHS-M2 showed good selectivity for Na_2S over other biologically relevant reactive sulfur (RSS), oxygen (ROS), and nitrogen species (RNS) (Figure 2). Both probes displayed 5−8-fold greater response for H_2S over 10 mM glutathione (GSH) (100-fold larger amount than H_2S tested), 1 mM cysteine (Cys), and 1 mM 2-mercaptoethanol (2-ME). Moreover, these probes displayed strong response upon addition of 100 μM Na_2S in the presence of GSH (10 mM) or Cys (1 mM) (Figure 2), thereby conforming the high selectivity for H_2S over GSH and Cys. Other biologically relevant RSS (lipoic acid, SO_3^{2-}, $S_2O_3^{2-}$, SCN^-), RNS (NO_2^-, NO), ROS (H_2O_2, O_2^-, *t*-BuOOH, HOCl), amino acids without thiol groups (Ala, Glu), and metal ions (Ca^{2+}, K^+, Na^+, Fe^{3+}, Zn^{2+}, Mg^{2+}) showed negligible responses (Figure 2). Furthermore, SHS-M1 and SHS-M2 were pH-insensitive over a biologically relevant pH range (Figure S6 in the SI). Therefore, these probes can detect intracellular sulfide with minimum interference from other biologically relevant analytes and pH.

dx.doi.org/10.1021/ja404004v | *J. Am. Chem. Soc.* 2013, 135, 9915−9923

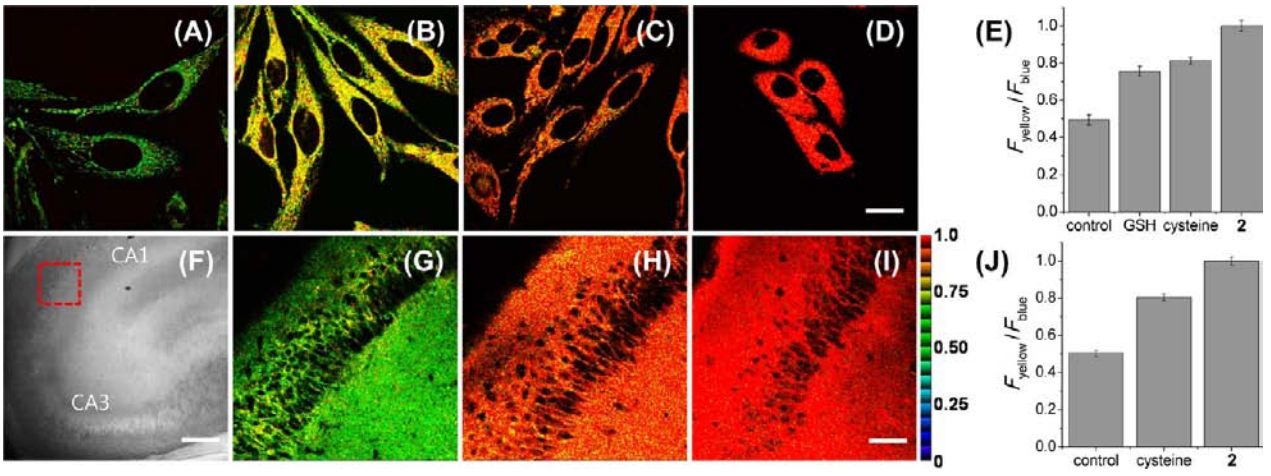

Figure 3. (A–D) Pseudocolored ratiometric TPM images (F_{yellow}/F_{blue}) of (A, D) HeLa cells incubated with 2 μM (A) SHS-M2 or (D) **2** and (B, C) HeLa cells pretreated with 100 μM (B) GSH or (C) cysteine for 30 min before labeling with SHS-M2. Images were acquired using 750 nm excitation and emission windows of 425–470 nm (blue) and 525–575 nm (yellow). Cells shown are representative images from replicate experiments (n = 5). (E) Average values of F_{yellow}/F_{blue} in (A–D). (F) Bright-field images of the CA1 and CA3 regions of a rat hippocampal slice. (G–I) Ratiometric TPM images of fresh rat hippocampal slices stained with (G, H) 20 μM SHS-M2 for 1 h without (G) or with (H) pretreatment with 1 mM cysteine for 1 h and (I) 20 μM **2** for 1 h. TPM images were acquired at a depth of 120 μm with 40× magnification. (J) Average F_{yellow}/F_{blue} intensity ratios in (G–I). The TP fluorescence emission was collected in two channels (blue = 425–470 nm and yellow = 525–575 nm) upon excitation at 750 nm with femtosecond pulses. Scale bars: (D) 20 μm; (F) 300 μm; (I) 75 μm.

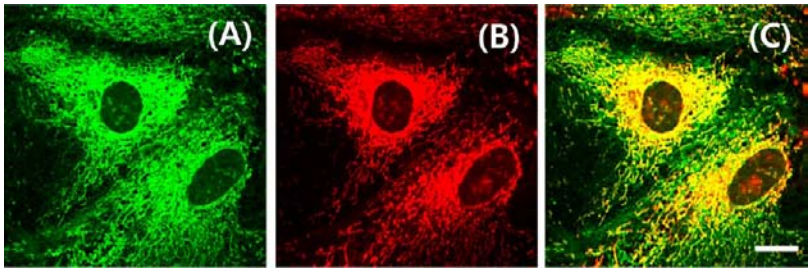

Figure 4. (A) TPM and (B) OPM images of astrocytes colabeled with (A) SHS-M2 and (B) MitoTracker Red FM. (C) Merged image. The wavelengths for TP and OP excitation were 750 and 514 nm, respectively, and the corresponding emissions were collected at 425–575 nm (SHS-M2) and 600–700 nm (Mitotracker Red FM). Scale bar = 30 μm. Cells shown are representative images from replicate experiments (n = 3).

The TP action cross sections ($\Phi\delta_{max}$, where δ is the TP absorption cross section) were determined by investigating the TPEF spectra with rhodamine 6G as the reference (see the SI).[23] The $\Phi\delta_{max}$ values for SHS-M1, **1**, SHS-M2, and **2** were 14, 63, 17, and 55 GM, respectively (1 GM = 10^{-50} cm^4 s photon^{-1}; Table 1 and Figure S7 in the SI). The larger values for **1** and **2** than for SHS-M1 and SHS-M2 can be attributed to the enhanced donor and acceptor abilities, respectively[24] (Table 1). In EtOH, which is a good model for the cellular environment (vide supra), the $\Phi\delta_{max}$ values for SHS-M2 and **2** were 1.9–2.3-fold larger than those for SHS-M1 and **1**. Indeed, the TPM images of the cells labeled with SHS-M2 were much brighter than those labeled with SHS-M1, while both probes showed high photostability (Figure S8 in the SI). Moreover, the emission intensity of SHS-M2 in EtOH increased gradually at 510 nm with a concomitant decrease at 445 nm in the presence of excess Na_2S with k_2 = 4.6 M^{-1} s^{-1}, a result similar to that observed in HEPES buffer (Figure S9 in the SI). The value of F_{yellow}/F_{blue}, the ratio of the relative emission intensities at 525–575 nm (F_{yellow}) and 425–470 nm (F_{blue}), showed a 9-fold increase, establishing that SHS-M2 can serve as a ratiometric fluorescence probe for H_2S in cells. Therefore, we used SHS-M2 in the imaging experiments.

Detection of Mitochondrial H_2S with SHS-M2 in Live Cells and Tissue. We then tested the utility of SHS-M2 to detect H_2S in the cellular environment. TPM image of HeLa cells labeled with SHS-M2 was bright (Figure 3A), presumably because of the easy loading, convenient rate of H_2S-induced reduction, and large $\Phi\delta_{max}$ value of the reaction product. To confirm whether the probes could specifically stain the mitochondria, HeLa cells were stained with SHS-M2 and MitoTracker Red (MTR),[25] a well-known one-photon-fluorescence marker for mitochondria. The TPM image of SHS-M2 merged well with the one-photon microscopy (OPM) image of MTR (Figure S10 in the SI). The Pearson's colocalization coefficient[26] of SHS-M2 and MTR was A = 0.85 as calculated using Autoquant X2 software, indicating that SHS-M2 existed predominantly in the mitochondria. An experiment in astrocytes gave a similar result with A = 0.82 (Figure 4). Furthermore, SHS-M2 showed low cytotoxicity as determined using a CCK-8 kit (Figure S11 in the SI).

Next, we tested whether SHS-M2 can monitor the changes in mitochondrial H_2S levels in live cells and tissues. Upon TP excitation at 750 nm, the average emission ratios (F_{yellow}/F_{blue}) of HeLa cells labeled with SHS-M2 and **2** were 0.49 and 1.00, respectively (Figure 3A,D,E and Figure S12 in the SI). The ratio increased from 0.49 to 0.76 or 0.81, respectively, after

dx.doi.org/10.1021/ja404004v | J. Am. Chem. Soc. 2013, 135, 9915–9923

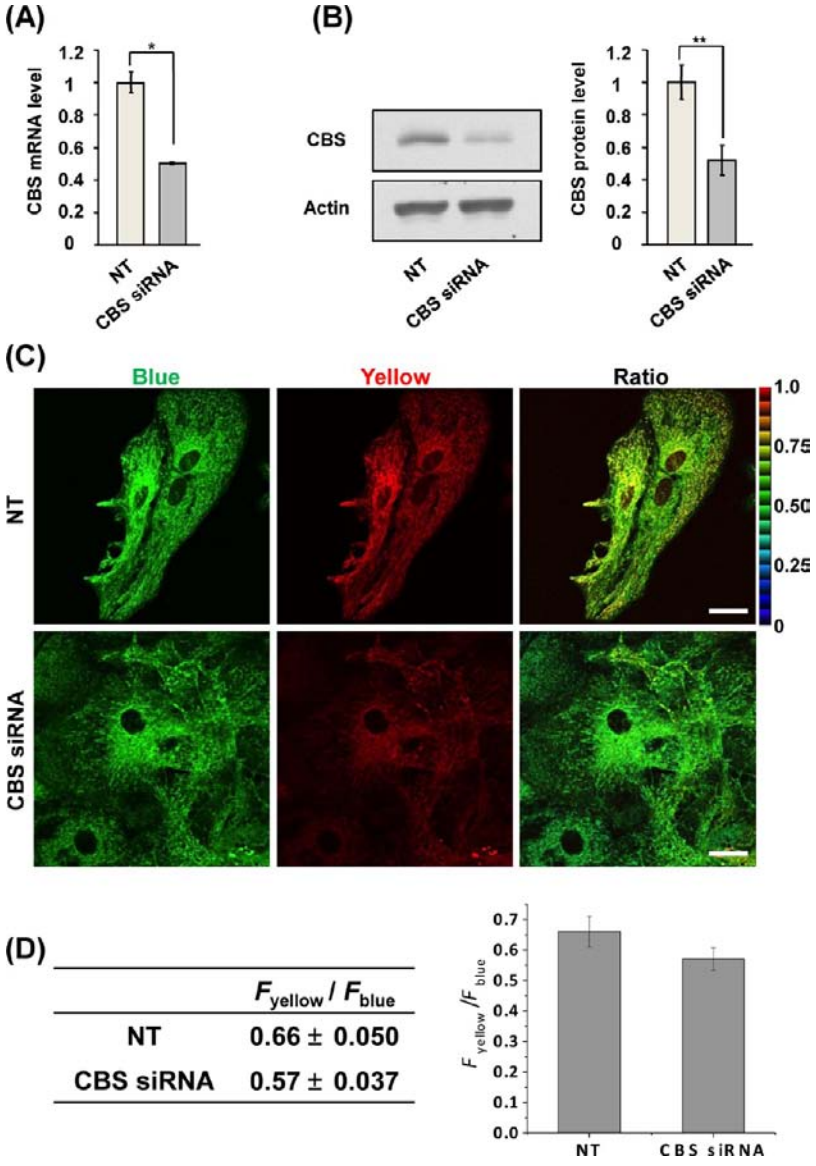

Figure 5. SHS-M2 showed a correlation between the CBS expression level and the amount of H_2S production. (A, B) Astrocytes prepared from neonate mice brain were treated with CBS-specific siRNA (20 nM) or nontargeted (NT) siRNA for 5 days. CBS mRNA levels (A) and protein levels (B) were analyzed with Q-PCR and Western blot, respectively, and quantified (B). (C) Astrocytes treated with CBS-specific or NT siRNA were stained with 2 μM SHS-M2 for 1 h. Images were acquired using 750 nm excitation and emission windows of 425−470 nm (blue) and 525−575 nm (yellow). (D) Average intensity ratios (F_{yellow}/F_{blue}) in TPM images calculated as described above. Each value in (A) and (B) is the mean ± standard error of the mean (SEM) of three samples, and each value in (D) is the mean ± standard deviation (SD) of three samples. Cells shown in (C) are representative images from replicate experiments (n = 3). Scale bar in (C) = 20 μm.

addition of GSH or Cys, which are the precursors to H_2S.[5b,27,28] Furthermore, we investigated the utility of SHS-M2 in a fresh rat hippocampal slice. We accumulated 10 TPM images at depths of 90−180 μm to visualize the overall H_2S distribution. They revealed that H_2S is more or less evenly distributed in both the CA1 and CA3 regions (Figures S13 and S14 in the SI) as well as at different depths. Moreover, a higher-magnification image clearly showed the H_2S distribution in the individual cells in the CA1 region with an average emission ratio of 0.51 at a depth of 120 μm (Figure 3G,J). The F_{yellow}/F_{blue} ratio increased to 0.80 when the tissue was treated with 1 mM cysteine for 50 min (Figure 3H,J). These results confirm that SHS-M2 is clearly capable of monitoring the endogenous H_2S levels in live cells and at >100 μm depth in living tissues using TPM.

Measurement of H_2S Levels in Cultured Astrocytes with SHS-M2. We next investigated whether SHS-M2 can measure H_2S levels in astrocytes produced by different levels of CBS, the major enzyme that catalyzes H_2S production. It is well-established that astrocytes express CBS and produce H_2S in the brain.[2,11,12] We knocked out CBS from astrocytes using CBS siRNA (5′-CCC AAA AUU UUA CCA GAU AUU CUU U-3′). Astrocytes pretreated with CBS siRNA for 5 days showed significantly reduced CBS mRNA and CBS protein levels compared with cells pretreated with nontargeted (NT) siRNA (5′-CCU CGU GCC GUU CCA UCA GGU AGU U-3′) (Figure 5A,B). Moreover, the F_{yellow}/F_{blue} ratio of SHS-M2-labeled astrocytes decreased from 0.66 to 0.56 when pretreated with NT-siRNA and CBS siRNA, respectively, indicating a parallel decrease in the H_2S levels (Figure 5C,D). This result

dx.doi.org/10.1021/ja404004v | J. Am. Chem. Soc. 2013, 135, 9915−9923

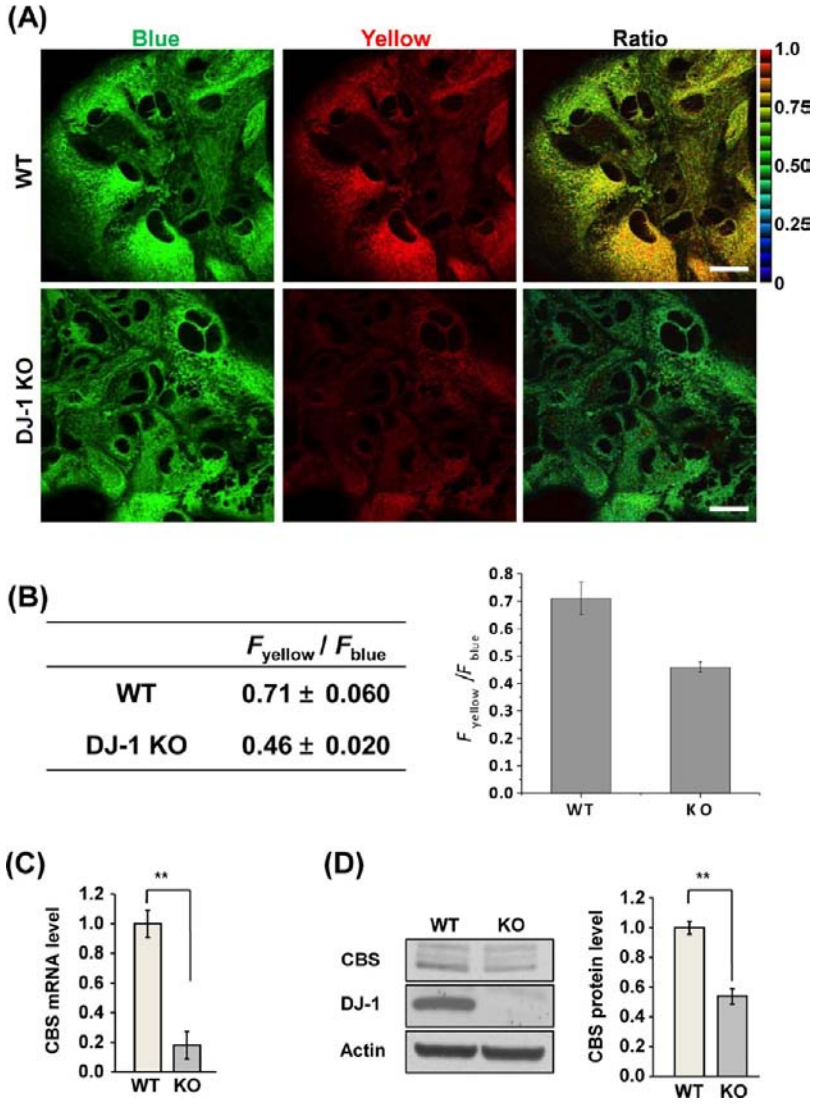

Figure 6. Attenuated H_2S production and CBS expression in DJ-1-KO astrocytes. (A, B) Astrocytes cultured from WT and DJ-1-KO mice brains were stained with 20 μM SHS-M2 for 1 h. (A) Ratiometric TPM images of the astrocytes revealed decreased H_2S production in the KO astrocytes compared with WT cells. (B) Average F_{yellow}/F_{blue} intensity ratios in the TPM images calculated as described above. (C, D) CBS mRNA (C) and protein levels (D) in WT and KO astrocytes were determined with Q-PCR and Western blot, respectively. Values in (B) are means ± SD of three samples, and values in (C) and (D) are means ± SEM of three samples. Scale bar in (A) = 20 μm.

demonstrates the capability of SHS-M2 to delineate the relationship between the CBS expression level and the H_2S level in astrocytes by TPM.

Measurement of Endogenous H_2S Levels in DJ-1-Deficient Astrocytes and Brain Slices. We then utilized SHS-M2 to measure the endogenous H_2S levels in DJ-1-deficient astrocytes and mouse brain slices. DJ-1 is a PD-related gene that has multiple functions. It was reported that DJ-1 exerts anti-inflammatory and antioxidant effect in astrocytes.[29−32] Since H_2S also has anti-inflammatory and antioxidant effects,[4,10,11] it was interesting to find out whether DJ-1 regulates H_2S production. Using SHS-M2 as the probe, we found that the F_{yellow}/F_{blue} ratio in DJ-1-knockout (KO) astrocytes decreased to 0.46 from 0.71 measured in wild-type (WT) astrocytes (Figure 6A,B). This outcome indicates a parallel decrease in the endogenous H_2S level. Moreover, the CBS mRNA and CBS protein levels were significantly reduced in DJ-1-KO astrocytes compared to WT astrocytes (Figure 6C,D). Here again, a parallel decrease in the CBS expression level and the endogenous H_2S level is clearly indicated.

We further investigated the relationship between CBS expression and H_2S production in WT and DJ-1-KO brain slices. Slices were freshly prepared from WT and KO brain hippocampus and double-stained with antibodies specific for GFAP (an astrocyte marker) and CBS, respectively. As expected, CBS was detected in GFAP-positive astrocytes, and its expression was dramatically reduced in DJ-1-KO astrocytes (Figure 7A). H_2S was also detected in cells having astrocyte morphology (Figure 7B) and was significantly reduced in DJ-1-KO slices compared with WT slices (Figure 7B,C). We then analyzed H_2S production in cortical slices 7 days after slicing to stabilize the tissues from slicing stress.[33] The ratiometric images of SHS-M2-labeled tissues showed reduced H_2S levels in DJ-1-KO cortical slices (Figure 7D,E), as observed in cultured astrocytes (Figure 6) and freshly prepared slices (Figure 7B,C). These results indicate that TPM ratiometric imaging using SHS-M2 as the probe is an effective tool for measuring different

dx.doi.org/10.1021/ja404004v | J. Am. Chem. Soc. 2013, 135, 9915−9923

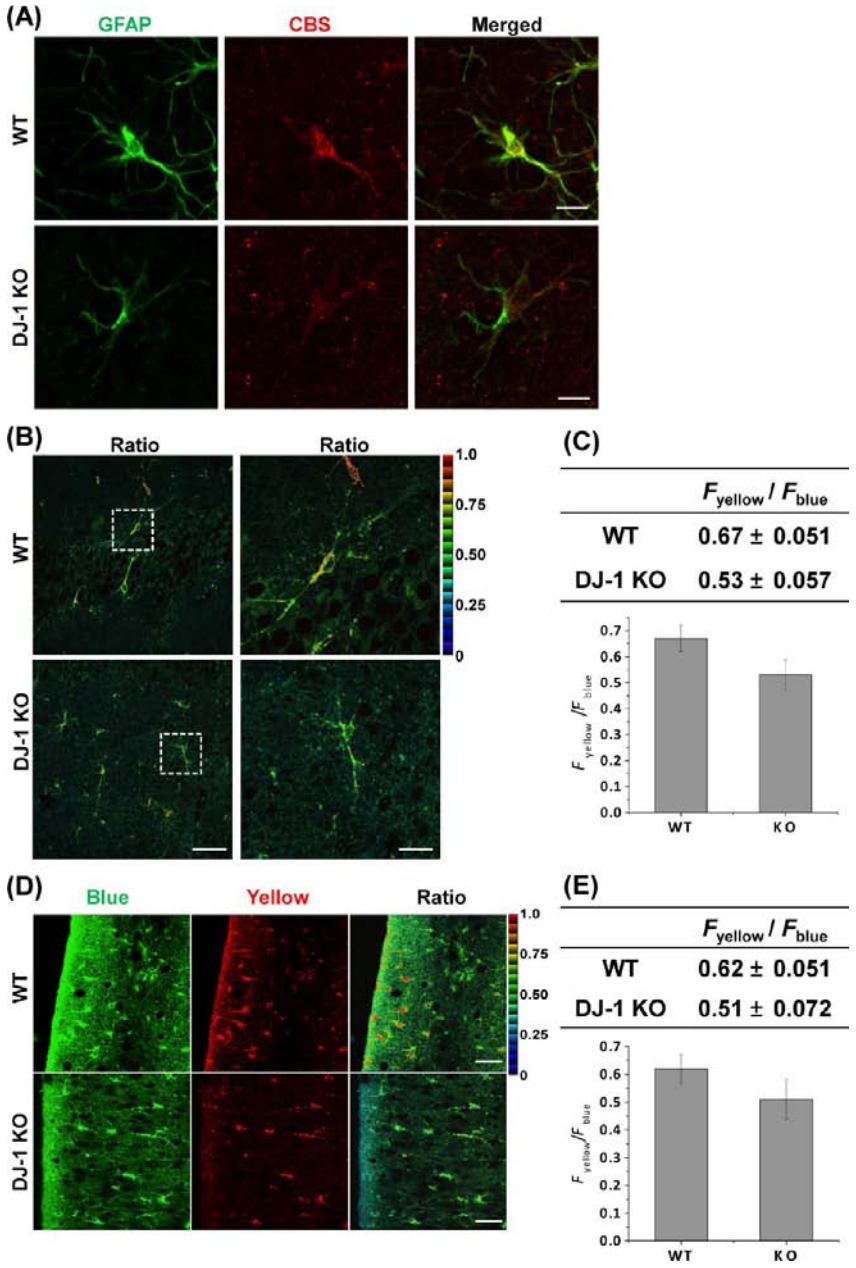

Figure 7. Attenuated CBS expression and H_2S production in astrocytes in DJ-1-KO brain. Brain slices were prepared from WT and DJ-1-KO mice. (A–C) Hippocampal slices were acutely prepared and used for (A) GFAP and CBS staining as described in the Experimental Section or (B, C) H_2S analysis as described above. In (B), the right panels show higher-magnification images of boxed areas in the left panels. (D, E) Cortical slices were cultured for 7 days after slicing to stabilize the tissues from slicing stress, and then the H_2S production was measured. Values in (C) and (E) are means ± SD of three samples. Scale bars: (A) 30 μm; (B) (left) 75 μm, (right) 30 μm; (D) 75 μm.

H_2S levels produced by different CBS expression levels. To the best of our knowledge, this is the first report showing that genetically mutated PD genes can affect H_2S production in PD patients' brains, partially in astrocytes.

Concluding Remarks. In this work, we have developed SHS-M2, a new mitochondrial-specific and emission-ratiometric TPM probe for H_2S that shows a significant TP cross section, a marked blue-to-yellow emission color change in response to H_2S, high mitochondrial H_2S selectivity, high photostability, low cytotoxicity, and good performance over the biologically relevant pH range. This probe can ratiometrically detect mitochondrial H_2S in live cells and living tissues for a long period of time by TPM with minimum interference from other biologically relevant species.

In addition, TPM ratiometric imaging using SHS-M2 as the probe is an effective tool for measuring different H_2S levels produced by different expression levels of CBS in WT and DJ-1-KO astrocytes and brain slices. These findings demonstrate that H_2S levels decrease in a genetic model of PD. Furthermore, SHS-M2 may find useful applications in biomedical research including PD through the use of TPM.

■ EXPERIMENTAL SECTION

Spectroscopic Measurements. Absorption spectra were recorded on an S-3100 UV–vis spectrophotometer, and fluorescence spectra were obtained with a FluoroMate FS-2 fluorescence spectrophotometer with a 1 cm standard quartz cell. The fluorescence

dx.doi.org/10.1021/ja404004v | J. Am. Chem. Soc. 2013, 135, 9915–9923

quantum yield was determined by the literature method[34] using coumarin 307 (Φ = 0.95 in MeOH) as the reference

Measurement of Two-Photon Cross Section. The two-photon absorption (TPA) cross section (δ) was determined by the femtosecond fluorescence measurement technique as described elsewhere.[35] Dye (1.0×10^{-6} M) was dissolved in 30 mM HEPES buffer (pH 7.4), and the TP-induced fluorescence intensity was measured at 720−880 nm using rhodamine 6G as the reference, whose TP properties have been well-characterized in the literature.[36] The intensities of the TP-induced fluorescence spectra of the reference and sample emitted at the same excitation wavelength were determined. The TPA cross section was calculated as $\delta = \delta_r(S_s\Phi_r\phi_r c_r)/(S_r\Phi_s\phi_s c_s)$, where the subscripts s and r stand for the sample and reference molecules, respectively, S is the intensity of the signal collected by the CCD detector, Φ is the fluorescence quantum yield, ϕ is the overall fluorescence collection efficiency of the experimental apparatus, and c is the number density of the molecules in solution.

Animals. The DJ-1-KO mice used in this study were a gift from U. J. Kang (University of Chicago). DJ-1-KO mice were previously generated by deleting 9.3 kb of genomic DNA, including the first five exons and part of the promoter region of the DJ-1 gene.[37]

Cell Culture. HeLa human cervical carcinoma cells (ATCC, Manassas, VA, USA) were cultured in Dulbecco's modified Eagle's medium (DMEM) (WelGene Inc., Seoul, Korea) supplemented with 10% fetal bovine serum (FBS) (WelGene), penicillin (100 units/mL), and streptomycin (100 μg/mL). Two days before imaging, the cells were passed and plated on glass-bottomed dishes (NEST). All of the cells were maintained in a humidified atmosphere of 5/95 (v/v) CO_2/air at room temperature. For labeling, the growth medium was removed and replaced with DMEM without FBS. The cells were treated and incubated with 2 μM SHS-M1, **1**, SHS-M2, or **2** at 37 °C under 5% CO_2 for 30 min. The cells were washed three times with phosphate-buffered saline (PBS) (Gibco) and then imaged after further incubation in colorless serum-free medium for 30 min.

Primary astrocytes were cultured from the cortex of DJ-1-KO or WT mice brains. In brief, cortexes were removed and triturated in DMEM (Invitrogen, Carlsbad, CA, USA) containing 10% FBS (HyClone, Logan, UT, USA), plated in 75 cm^2 T-flasks (0.5 hemisphere/flask), and incubated for 2−3 weeks. Microglia were detached from flasks by mild shaking, filtered through a nylon mesh to remove cell clumps, and cultured in DMEM containing 10% FBS.[38] Astrocytes remaining in the flask were harvested with 0.1% trypsin and cultured in DMEM containing 10% FBS. BV2 murine microglia were cultured in DMEM containing 5% FBS as described previously.[39] For activation of glial cells, cells were treated with 5 ng/mL recombinant murine IFN (PeproTech, Rocky Hill, NJ, USA).

Preparation and Staining of Fresh Rat Hippocampal Slices. Rat hippocampal slices were prepared from the hippocampi of 2-week-old rat (SD) according to an approved institutional review board protocol. Coronal slices with a thickness of 400 μm were cut using a vibrating-blade microtome in artificial cerebrospinal fluid (ACSF) (124 mM NaCl, 3 mM KCl, 26 mM $NaHCO_3$, 1.25 mM NaH_2PO_4, 10 mM D-glucose, 2.4 mM $CaCl_2$, and 1.3 mM $MgSO_4$). The slices were incubated with 20 μM SHS-M2 in ACSF bubbled with 95% O_2 and 5% CO_2 for 1 h 30 min at 37 °C, washed three times with ACSF, transferred to glass-bottomed dishes (NEST), and observed in a spectral confocal multiphoton microscope.

Organotypic Cortical Slice Cultures. Cortical slices were prepared according to a modified version of a previously described protocol.[40] Slices were obtained from postnatal day 7 mice. Briefly, the brains were rapidly removed and the cortices separated by thin forceps in culture medium. Coronal cortical slices (400 μm thick) were prepared using a McIlwain tissue chopper (Mickle Laboratory Engineering, Goose Green, UK). Slices were placed on membranes (0.4 mm pore size) of inserts (Millipore, Cork, Ireland). Each well was filled with slice culture medium [minimum essential medium (MEM) containing 25% (v/v) Hanks' balanced salt solution, 25% (v/v) heat-inactivated horse serum (HyClone), 6.5 mg/mL glucose, 1 mM L-glutamine, 10 units/mL penicillin-G, and 10 mg/mL streptomycin]. For stabilization, slices were incubated for 7 days with the medium changed on days 3 and 5. On day 7, slices were used for experiments.

siRNA Transfection. CBS protein expression in astrocytes was knocked out using CBS-specific siRNA (Genolution Phamaceuticals, Seoul, Korea). The sequence of the CBS-specific siRNA was 5′-CCC AAA AUU UUA CCA GAU AUU CUU U-3′, and the sequence of the nontargeted siRNA sequence was 5′-CCU CGU GCC GUU CCA UCA GGU AGU U-3′. For siRNA transfection, astrocytes were placed in Opti-MEM (Invitrogen, Carlsbad, CA, USA) and treated with 20 nM siRNA and RNAiMAX transfection reagent. After 4 h, the astrocytes were placed in 10% FBS-containg DMEM and incubated for 5 days. Reduced CBS expression was confirmed using qPCR and Western blot.

Quantitative Real-Time PCR. CBS mRNA expression was analyzed using quantitative real-time PCR (qPCR). In brief, total RNA was isolated using RNAzol B (iNtRON, Sungnam, Korea), and complementary DNA was prepared using Avian Myeloblastosis Virus reverse transcriptase (Promega, Madison, WI, USA) according to the manufacturer's protocol. qPCR was done using 2× KAPA SYBR Fast Master Mix (Kapa Biosystems, Cape Town, South Africa) and an RG-6000 real-time amplification instrument (Corbett Research, Sydney, Australia). The qPCR primer sets specific for CBS were 5′-CCA TGG CTG TGG CTG TGA A-3′ (sense) and 5′-CCA TTT GTC ACT CAG GAA CTT GGA-3′ (antisense), and those for actin were 5′-GCT CTG GCT CCT AGC ACC AT-3′ (sense) and 5′-GCC ACC GAT CCA CAC AGA GT-3′ (antisense). Actin was used as a reference gene. The threshold cycle values of each of the genes were presented as relative fold induction.

Western Blot. Astrocytes were washed with cold PBS and lysed with RIPAa buffer (1% NP-40, 150 mL NaCl, 10 mM Na_2HPO_4, pH 7.2, 0.5% sodium deoxycholate) containing protease inhibitors (2 mM PMSF, 10 μg/L leupeptin, 10 μg/L pepstatin, and 0.5 mM $NaVO_3$). Proteins were separated by 10% sodium dodecyl sulfate polyacrylamide gel electrophoresis (SDS-PAGE) and transferred to nitrocellulose membranes. The membranes were incubated with 5% nonfat milk to block nonspecific antibody binding and then with antibodies specific for CBS (1:1000; Santa Cruz Biotechnology, Santa Cruz, CA, USA), DJ-1 (1:1000; Cell Signaling Technology, Beverly, MA, USA), or β-actin (1:1000; Santa Cruz Biotechnology). Membranes were washed, incubated with peroxidase-conjugated secondary antibodies (1:10000; Zymed, San Fransico, CA, USA), and visualized using an enhanced chemiluminescence (ECL) system (BioNote, Gyeonggi, Korea).

Immunohistochemistry. For immunofluorescence staining, slices and/or brain sections were obtained, washed three times in PBS containing 0.2% Triton X-100 (PBST). Nonspecific antibody binding was blocked with 1% BSA in PBST. Slices and/or sections were incubated with specific antibodies for GFAP (1:50; Cell Signaling Technology) or CBS (1:50; Santa Cruz Biotechnology). After washing, slices and/or sections were incubated with secondary antibodies conjugated with Alexa Fluor 488 or Alexa Fluor 555 (1600 dilution; Invitrogen, Eugene, OR, USA). 4',6-Diamidino-2-phenylindole (DAPI) (Vector Laboratories, Burlingame, CA, USA) was used to detect nuclei. All of the samples were analyzed under a confocal microscope (Carl Zeiss, Germany) with 63× oil immersion objectives.

Two-Photon Fluorescence Microscopy. Two-photon fluorescence microscopy images of cells and tissues labeled with SHS-M1, **1**, SHS-M2, or **2** were obtained with spectral confocal and multiphoton microscopes (Leica TCS SP8MP) with 10× dry, 40× oil, 63× oil, and 100× oil objectives [numerical aperture (NA) = 0.30, 0.30, 1.40, and 1.30, respectively]. The two-photon fluorescence microscopy images were obtained with a DMI6000B microscope (Leica) by exciting the probes with a mode-locked titanium−sapphire laser source (MaiTai Spectra Physics, 80 MHz, 100 fs) set at a wavelength of 750 nm and an output power of 2710 mW, corresponding to an average power of approximately 10 mW in the focal plane. To obtain images at 425−575 nm, internal photomultiplier tubes were used to collect the signals in an 8 bit unsigned 512 × 512 and 1024 × 1024 pixels at scan speeds of

400 and 200 Hz, respectively. Ratiometric image processing and analysis was carried out using MetaMorph software.

■ ASSOCIATED CONTENT

Supporting Information

Synthesis, additional methods, Figures S1−S20, and Table S1. This material is available free of charge via the Internet at http://pubs.acs.org.

■ AUTHOR INFORMATION

Corresponding Author

ehjoe@ajou.ac.kr; chobr@korea.ac.kr; kimhm@ajou.ac.kr

Author Contributions

‖S.K.B., C.H.H., and D.J.C. contributed equally.

Notes

The authors declare no competing financial interest.

■ ACKNOWLEDGMENTS

National Research Foundation (NRF) grants funded by the Korean Government (20120008780 and 2012007850), the Priority Research Centers Program through the NRF (20120006687 and 20120005860), and NRF through the Chronic Inflammatory Disease Research Center (CIDRC) at Ajou University (NRF-2012R1A5A2051429) are acknowledged.

■ REFERENCES

(1) Kimura, H. *Amino Acids* **2011**, *41*, 113.
(2) Abe, K.; Kimura, H. *J. Neurosci.* **1996**, *16*, 1066.
(3) Kabil, O.; Banerjee, R. *J. Biol. Chem.* **2010**, *285*, 21903.
(4) Zanardo, R. C.; Brancaleone, V.; Distrutti, E.; Fiorucci, S.; Cirino, G.; Wallace, J. L. *FASEB J.* **2006**, *20*, 2118.
(5) (a) Kimura, Y.; Goto, Y.; Kimura, H. *Antioxid. Redox Signaling* **2010**, *12*, 1. (b) Shibuya, N.; Tanaka, M.; Yoshida, M.; Ogasawara, Y.; Togawa, T.; Ishii, K.; Kimura, H. *Antioxid. Redox Signaling* **2009**, *11*, 703.
(6) (a) Mari, M.; Morales, A.; Colell, A.; Garcia-Ruiz, C.; Fernandez-Checa, J. C. *Antioxid. Redox Signaling* **2009**, *11*, 2685. (b) Cheng, W. Y.; Tong, H.; Miller, E. W.; Chang, C. J.; Remington, J.; Zucker, R. M.; Bromberg, P. A.; Samet, J. M.; Hofer, T. P. *Environ. Health Perspect.* **2010**, *118*, 902.
(7) (a) Pun, P. B.; Lu, J.; Kan, E. M.; Moochhala, S. *Mitochondrion* **2010**, *10*, 83. (b) Fu, M.; Zhang, W.; Wu, L.; Yang, G.; Li, H.; Wang, R. *Proc. Natl. Acad. Sci. U.S.A.* **2012**, *109*, 2943.
(8) Warenycia, M. W.; Goodwin, L. R.; Benishin, C. G.; Reiffenstein, R. J.; Francom, D. M.; Taylor, J. D.; Dieken, F. P. *Biochem. Pharmacol.* **1989**, *38*, 973.
(9) Goodwin, L. R.; Francom, D.; Dieken, F. P.; Taylor, J. D.; Warenycia, M. W.; Reiffenstein, R. J.; Dowling, G. *J. Anal. Toxicol.* **1989**, *13*, 105.
(10) Hu, L. F.; Lu, M.; Tiong, C. X.; Dawe, G. S.; Hu, G.; Bian, J. S. *Aging Cell* **2010**, *9*, 135.
(11) Lee, M.; Schwab, C.; Yu, S.; McGeer, E.; McGeer, P. L. *Neurobiol. Aging* **2009**, *30*, 1523.
(12) Eto, K.; Asada, T.; Arima, K.; Makifuchi, T.; Kimura, H. *Biochem. Biophys. Res. Commun.* **2002**, *293*, 1485.
(13) (a) Lippert, A. R.; New, E. J.; Chang, C. J. *J. Am. Chem. Soc.* **2011**, *133*, 10078. (b) Peng, H.; Cheng, Y.; Dai, C.; King, A. L.; Predmore, B. L.; Lefer, D. J.; Wang, B. *Angew. Chem., Int. Ed.* **2011**, *50*, 9672. (c) Chen, S.; Chen, Z.; Ren, W.; Ai, H.-W. *J. Am. Chem. Soc.* **2012**, *134*, 9589.
(14) Sasakura, K.; Hanaoka, K.; Shibuya, N.; Mikami, Y.; Kimura, Y.; Komatsu, T.; Ueno, T.; Terai, T.; Kimura, H.; Nagano, T. *J. Am. Chem. Soc.* **2011**, *133*, 18003.
(15) (a) Qian, Y.; Karpus, J.; Kabil, O.; Zhang, S. Y.; Zhu, H. L.; Banerjee, R.; Zhao, J.; He, C. *Nat. Commun.* **2011**, *2*, 495. (b) Liu, C.; Pan, J.; Li, S.; Zhao, Y.; Wu, L. Y.; Berkman, C. E.; Whorton, A. R.; Xian, M. *Angew. Chem., Int. Ed.* **2011**, *50*, 10327.
(16) Chen, Y.; Zhu, C.; Yang, Z.; Chen, J.; He, Y.; Jiao, Y.; He, W.; Qiu, L.; Cen, J.; Guo, Z. *Angew. Chem., Int. Ed.* **2013**, *52*, 1688.
(17) (a) Helmchen, F.; Denk, W. *Nat. Methods* **2005**, *2*, 932. (b) Zipfel, W. R.; Williams, R. M.; Webb, W. W. *Nat. Biotechnol.* **2003**, *21*, 1369.
(18) (a) Kim, H. M.; Cho, B. R. *Acc. Chem. Res.* **2009**, *42*, 863. (b) Kim, H. M.; Cho, B. R. *Chem.—Asian J.* **2011**, *6*, 58. (c) Sumalekshmy, C.; Fahrmi, C. J. *Chem. Mater.* **2011**, *23*, 483. (d) Yao, S.; Belfield, K. D. *Eur. J. Org. Chem.* **2012**, 3199.
(19) (a) Li, L.; Ge, J.; Wu, H.; Xu, Q. H.; Yao, S. Q. *J. Am. Chem. Soc.* **2012**, *134*, 12157. (b) Rao, A. S.; Kim, D.; Nam, H.; Jo, H.; Kim, K. H.; Ban, C.; Ahn, K. H. *Chem. Commun.* **2012**, *48*, 3206. (c) Dong, X.; Yang, Y.; Sun, J.; Liu, Z.; Liu, B. F. *Chem. Commun.* **2009**, 3883.
(20) (a) Masanta, G.; Heo, C. H.; Lim, C. S.; Bae, S. K.; Cho, B. R.; Kim, H. M. *Chem. Commun.* **2012**, *48*, 3518. (b) Lim, C. S.; Masanta, G.; Kim, H. J.; Han, J. H.; Kim, H. M.; Cho, B. R. *J. Am. Chem. Soc.* **2011**, *133*, 11132. (c) Masanta, G.; Lim, C. S.; Kim, H. J.; Han, J. H.; Kim, H. M.; Cho, B. R. *J. Am. Chem. Soc.* **2011**, *133*, 5698.
(21) Griffin, R. J.; Evers, E.; Davison, R.; Gibson, A. E.; Layton, D.; Irwin, W. J. *J. Chem. Soc., Perkin Trans. 1* **1996**, 1205.
(22) The pK_1 (6.96) and pK_2 (12.90) values of H_2S predict that H_2S and HS^- are the predominant sulfide species in aqueous solution regardless of whether H_2S, NaHS, or Na_2S is used.
(23) Makarov, N. S.; Drobizhev, M.; Rebane, A. *Opt. Express* **2008**, *16*, 4029.
(24) Kim, H. M.; Cho, B. R. *Chem. Commun.* **2009**, 153.
(25) *A Guide to Fluorescent Probes and Labeling Technologies*, 10th ed.; Haugland, R. P., Ed.; Molecular Probes: Eugene, OR, 2005.
(26) Manders, E. M.; Stap, J.; Brakenhoff, G. J.; van Driel, R.; Aten, J. A. *J. Cell Sci.* **1992**, *103*, 857.
(27) (a) Singh, S.; Padovani, D.; Leslie, R. A.; Chiku, T.; Banerjee, R. *J. Biol. Chem.* **2009**, *284*, 22457. (b) Hosoki, R.; Matsuki, N.; Kimura, H. *Biochem. Biophys. Res. Commun.* **1997**, *237*, 527.
(28) (a) Griffith, O. W.; Bridges, R. J.; Meister, A. *Proc. Natl. Acad. Sci. U.S.A.* **1978**, *75*, 5405. (b) Kumar, T. R.; Wiseman, A. L.; Kala, G.; Kala, S. V.; Matzuk, M. M.; Lieberman, M. W. *Endocrinology* **2000**, *141*, 4270. (c) Lieberman, M. W.; Wiseman, A. L.; Shi, Z. Z.; Carter, B. Z.; Barrios, R.; Ou, C. N.; Chevez-Barrios, P.; Wang, Y.; Habib, G. M.; Goodman, J. C.; Huang, S. L.; Lebovitz, R. M.; Matzuk, M. M. *Proc. Natl. Acad. Sci. U.S.A.* **1996**, *93*, 7923.
(29) Waak, J.; Weber, S. S.; Waldenmaier, A.; Gorner, K.; Alunni-Fabbroni, M.; Schell, H.; Vogt-Weisenhorn, D.; Pham, T. T.; Reumers, V.; Baekelandt, V.; Wurst, W.; Kahle, P. J. *FASEB J.* **2009**, *23*, 2478.
(30) Cornejo Castro, E. M.; Waak, J.; Weber, S. S.; Fiesel, F. C.; Oberhettinger, P.; Schutz, M.; Autenrieth, I. B.; Springer, W.; Kahle, P. J. *J. Neural Transm.* **2010**, *117*, 599.
(31) Junn, E.; Taniguchi, H.; Jeong, B. S.; Zhao, X.; Ichijo, H.; Mouradian, M. M. *Proc. Natl. Acad. Sci. U.S.A.* **2005**, *102*, 9691.
(32) Ren, H.; Fu, K.; Wang, D.; Mu, C.; Wang, G. *J. Biol. Chem.* **2011**, *286*, 35308.
(33) Huuskonen, J.; Suuronen, T.; Miettinen, R.; van Groen, T.; Salminen, A. *J. Neuroinflammation* **2005**, *2*, 25.
(34) Demas, J. N.; Crosby, G. A. *J. Phys. Chem.* **1971**, *75*, 991.
(35) Lee, S. K.; Yang, W. J.; Choi, J. J.; Kim, C. H.; Jeon, S. J.; Cho, B. R. *Org. Lett.* **2005**, *7*, 323.
(36) Makarov, N. S.; Drobizhev, M.; Rebane, A. *Opt. Express* **2008**, *16*, 4029.
(37) Chen, L.; Cagniard, B.; Mathews, T.; Jones, S.; Koh, H. C.; Ding, Y.; Carvey, P. M.; Ling, Z.; Kang, U. J.; Zhuang, X. *J. Biol. Chem.* **2005**, *280*, 21418.
(38) Pyo, H.; Jou, I.; Jung, S.; Hong, S.; Joe, E. H. *Neuroreport* **1998**, *9*, 871.
(39) Min, K. J.; Jou, I.; Joe, E. *Biochem. Biophys. Res. Commun.* **2003**, *312*, 969.
(40) Stoppini, L.; Buchs, P. A.; Muller, D. *J. Neurosci. Methods* **1991**, *37*, 173.